RAPID COMMUNICATIONS

PHYSICAL REVIEW B VOLUME 44, NUMBER 7 15 AUGUST 1991-I

Hall effect in macroscopic ballistic four-terminal square structures

Y. Hirayama,* S. Tarucha, T. Saku, and Y. Horikoshi
NTT Basic Research Laboratories, Musashino-Shi, Tokyo 180, Japan
(Received 21 March 1991)

The Hall effect is studied for 10–30-μm size ballistic four-terminal square structures fabricated on an $Al_xGa_{1-x}As$-GaAs high-mobility modulation-doped wafer. On this scale, four-terminal square structures with sharp aperture corners are possible. The Hall resistance is not quenched and is larger than the classical linear value in a low magnetic field. It has periodic peaks corresponding to electron focusing when the terminals are narrow, and a broadening of these peaks makes a plateaulike structure when the terminals are wide.

Since Roukes *et al.*[1] found "quenching" of the Hall voltage in narrow one-dimensional (1D) wires, many interesting experiments and theories have been reported for the Hall effect in mesoscopic structures.[2–12] The deviation of Hall voltage from a classical linear line has been discussed in connection with the ballistic nature of the system. Chang and others[4–6] experimentally demonstrated that the "quenching," "last plateau," and "negative Hall effect" are explained by ballistic trajectories bouncing at boundaries. In these experiments, the size of the structure was around 1 μm and the actual boundary shape was considerably distorted by a depletion region spreading from lithographically defined boundaries. In such a situation, the collimation effect due to gradual widening of the wire especially has an important influence on the obtained characteristics. With a smaller system (a quantum dot with four leads), Ford *et al.*[11] recently observed resonant suppression of the quantized Hall effects, and Kirczenow and Castaño[12] explained this suppression as interference between different edge states. Behringer *et al.*[13] also found many features in the bend resistance[14] of a small four-terminal structure. These results indicate the important role of interference in small systems.

On the other hand, it is interesting to investigate a large but still ballistic structure, in which we can expect classical ballistic transport without interference and collimation. In this paper, we report Hall voltage characteristics of four-terminal square structures with square size between 10 and 30 μm. Even in such a large structure, the ballistic nature dominates transport characteristics when we use a high mobility two-dimensional (2D) electron gas at a heterointerface grown by a sophisticated molecular-beam epitaxy.[15–17] The sample shape used in this experiment is the same as the widened cross used by Ford *et al.*[5] However, the structure is an order of magnitude larger than theirs, so boundary shape distortion due to depletion region spreading becomes negligibly small. Therefore, the structure is considered to be a widened cross with rather sharp aperture corners. In addition, we discuss Hall characteristics for four-terminal square structures with various size parameters and shapes, which are determined exactly with an optical microscope.

Four-terminal square structures were chemically mesa-etched from a high mobility $Al_{0.35}Ga_{0.65}As$-GaAs modulation doped wafer (Fig. 1). The starting 2D electron gas has a carrier density n of 2.8×10^{11} cm^{-2} and a mobility μ of 7.8×10^{6} cm^2/Vs at 1.5 K after illumination. The detailed layer structure and growth condition are reported elsewhere.[16] The side length L ranged between 10 and 30 μm, and the width of terminal wire at each corner W was between 2.5 and 10 μm. The ratio L/W was varied from 3 to 10. Here, L and W were determined by optical microscope observation. Although rounding of the aperture corner by mesa-etching considerably distorted the shape for the structure with $L\leq10$ μm, the rounding effect is insignificant for the structure with $L\geq20$ μm [see Fig. 1(b)]. The ballistic mean free path of electrons in these structures was estimated to be around 80 μm at 1.5 K.[17] Therefore, ballistic properties dominated the transport characteristics, even for $L=30$ μm.

Hall voltage ($V_H=V_{24}$) was measured between terminals 2 and 4 with a constant dc of 250 nA applied between terminals 1 and 3 (I_{13}). For some structures, the bend resistance ($R_B=V_{43}/I_{12}$) was also measured in the same magnetic-field range. The value $I_{12}=0.5$–2 μA was used in this measurement. All measurements were made at 1.5 K in the dark after about 20 s of illumination. The injected current level was much larger than that conventionally used in mesoscopic experiments. This large current level comes from the wide terminals ($W\geq2.5$ μm) used in this experiment. The voltage applied between terminals 1 and 3 was still less than 100 μV for all Hall measurements and we can neglect any heating effects.

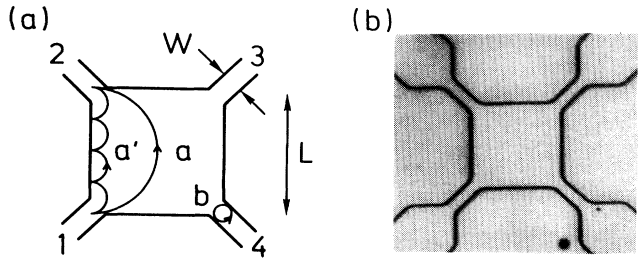

FIG. 1. (a) Schematic diagram of the high mobility four-terminal square structure. Trajectories a, a', and b correspond to B_{f1}, B_{fk} ($k=4$), and B_w. They are discussed in the text. (b) Optical micrograph of $(L,W)=(30,4.4)$(μm) sample.

Hall resistance ($R_H = V_{24}/I_{13}$) characteristics measured for structures with $L = 30$ μm and 3 μm $\leq W \leq 9.8$ μm and a structure with $L = 20$ μm and $W = 6.5$ μm are shown in Fig. 2. R_B characteristics for $L = 30$ μm and $W = 4.4$ and 9.8 μm are also shown in the figure. Though experimental results have some asymmetric characteristics probably originating from an impurity effect and/or an unintentional inhomogeneity between the terminal wires, they clearly indicate the following interesting behavior. (i) Quenching of R_H around $B = 0$ is not observed in Fig. 2, though a slight suppression of R_H is observed for $(L,W) = (20,6.5)$ and $(30,3)$(μm). On the other hand, the ballistic nature of the samples is confirmed by the clear observation of a negative resistance peak in R_B. (ii) R_H becomes larger than the classical linear value and makes a plateau between the magnetic field B_{f1} satisfying the relation of $B_{f1} = (8mE_F)^{1/2}/eL$ [trajectory a in Fig. 1(a)] and B_w satisfying $2l_{cyc}(B = B_w) = W$ [trajectory b in Fig. 1(a)]. Here, l_{cyc} is the cyclotron radius with $E_F = 9.8$ meV (corresponding to $n = 2.8 \times 10^{11}$ cm^{-2}). (iii) As the ratio L/W increases, the plateau separates into a series of focusing peaks at the field of $B_{fk} = (8mE_F)^{1/2}k/eL$ (k: integer).[18] These focusing characteristics are also observed in the magnetic-field dependence of R_B.

The rounding of the shape becomes important for $L = 10$ μm structures. The rounding can be enhanced under a lithographic condition slightly deviated from the optimum point. Typical characteristics of R_H and R_B for $L = 10$ μm structures are shown in Fig. 3 with optical micrographs and schematic drawings. In contrast with Fig. 2, suppression of R_H around $B = 0$ is apparent in Fig. 3.

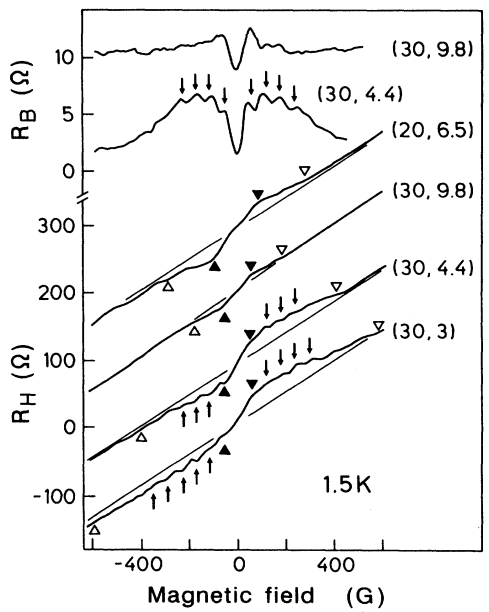

FIG. 2. R_H and R_B characteristics of four-terminal square structures with various (L,W) measured at 1.5 K ($L \geq 20$ μm). The R_H curves are offset vertically by 100 Ω and the R_B curves are offset by 10 Ω for clarity. Solid triangles, arrows, and open triangles indicate B_{f1}, B_{fk} (k: integer), and B_w, respectively. The classical linear Hall characteristics are indicated by fine-solid lines.

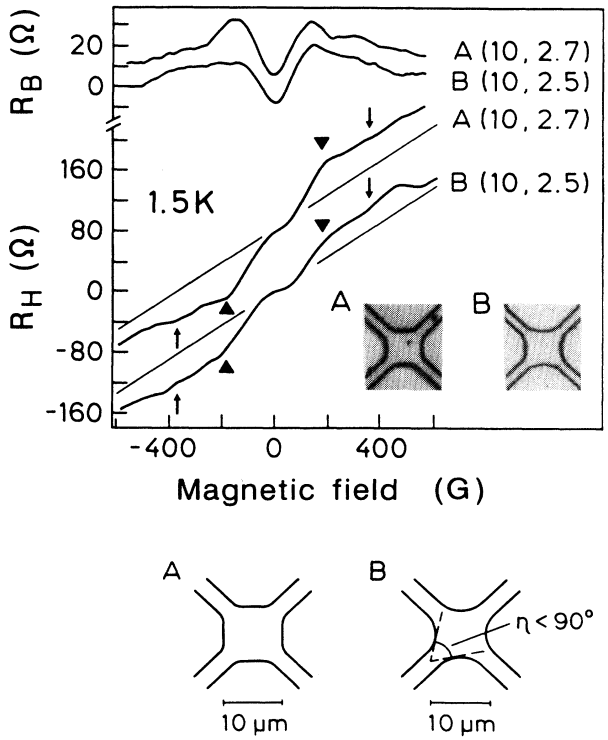

FIG. 3. R_H and R_B characteristics of $L = 10$ μm structures; A is a typical structure and B is an intentionally rounded structure. An optical micrograph of each structure is shown in the figure; bottom inset indicates a schematic drawing. Solid triangles, arrows, and fine-straight lines indicate B_{f1}, B_{fk} ($k = 2$), and classical linear R_H. The R_H curves are offset vertically by 80 Ω and the R_B curves are offset by 20 Ω for clarity.

Furthermore, suppression of R_H is enhanced for the more distorted (rounded) structure and R_H is almost quenched for the structure B in Fig. 3. On the other hand, the R_B characteristics are similar between these two samples. This indicates that a strong collimation with distinctly enhancing a straight injection does not occur in the structure, though a direct ballistic component from terminal 1 to 2 is shadowed around $B = 0$ by the round shape.

These results confirm that there is no suppression of R_H in the four-terminal structure (or the widened cross) with sharp aperture corners. The sharp corners prohibit an adiabatic injection and suppress the collimation effects. This forms a striking contrast to the widened cross of Ford *et al.*[5] where the smooth horn formed by depletion region produces a strong collimation. When there is no collimation for injection from terminal 1, $T_{21} > T_{41}$ is established at any applied magnetic field by the difference of the direct ballistic component between $1 \rightarrow 2$ and $1 \rightarrow 4$. Therefore, R_H expressed as[10,19]

$$R_H = \frac{h}{2e^2}\frac{1}{N}\frac{T_{21}-T_{41}}{T_{21}^2+T_{41}^2+2T_{31}(T_{31}+T_{21}+T_{41})} \quad (1)$$

is not quenched around $B = 0$. In Eq. (1), T_{ij} is the transmission probability from terminal j to i and N is a number of subbands in each terminal. When the injection around $\theta \sim 0$ is shadowed by the round shape and cannot

reach terminal 2, we can consider the injected angular distribution to be effectively limited to within $\frac{1}{4}\pi-\frac{1}{2}\eta < \theta < \frac{1}{4}\pi+\frac{1}{2}\eta$ $(\eta < \frac{1}{2}\pi)$ as shown in the bottom inset of Fig. 3. This distribution suppresses the direct ballistic components from 1 to both 2 and 4 in the magnetic-field region below $B_s=(8mE_F)^{1/2}\sin(\frac{1}{4}\pi-\frac{1}{2}\eta)/eL$. Assuming that scrambling trajectories make no difference between 2 and 4, $T_{21}=T_{41}$ and $R_H=0$. The values $B_s\sim 40$ G is obtained for the structure B shown in Fig. 3. This B_s approximately agrees with the width of the experimentally observed quenching region. These effects probably more or less remain in other structures and are responsible for the slight suppression of R_H observed in Fig. 2. It is noteworthy that we never observed a negative R_H in our experiments, including in the measurements of slightly rounded structures. This indicates that a strong collimation is essential for obtaining negative R_H due to "rebouncing."[7]

Finally, we show a simple calculation for explaining the obtained results. We assume the configuration shown in the top inset of Fig. 4(b). In real system with a finite ballistic mean free path, shorter trajectories have greater influence on the transport characteristics.[6] The path length of ballistic trajectories between 1 and 2 is shorter than that of complex scrambling trajectories. Then, a point injection source (1), collector (2), and a specular boundary between 1 and 2 are considered in place of a real four-terminal structure. The angular distribution of injection is assumed to be (I1) $\frac{1}{2}[\cos(\theta-\frac{1}{4}\pi)+|\sin(\theta-\frac{1}{4}\pi)|](0<\theta<\frac{1}{2}\pi)$, corresponding to an injection from perfectly sharp aperture corners, (I2) $(1/\sqrt{2})\times\cos(\theta-\frac{1}{4}\pi)(0<\theta<\frac{1}{2}\pi)$, corresponding to a conventional classical distribution without collimation, and (I3) $[1/2\sin(\eta/2)]\cos(\theta-\frac{1}{4}\pi)$ $(\frac{1}{4}\pi-\frac{1}{2}\eta<\theta<\frac{1}{4}\pi+\frac{1}{2}\eta;\eta=\frac{5}{18}\pi)$, corresponding to a slightly collimated or shadowed injection. The probability f that trajectories injected from 1 are ballistically collected in terminal 2 is calculated as a function of magnetic field and shown in the insets of Fig. 4. When L/W is large, f clearly indicates a peak structure corresponding to focusing. The peak structure is not so pronounced as in a normal focusing experiment configuration[18] because of the competition of the $\theta=\frac{1}{4}\pi$ injection component and the $\theta=\frac{1}{2}\pi$ focusing component in this configuration.[9] The latter produces peaks at the field of $B_{fk}=(8mE_F)^{1/2}k/eL$ (k: integer). When f is large ($f>0.5$), we can assume for the four-terminal structure that $T_{21}=f$, $T_{31}=1-f$, and $T_{41}=0$. Thus, R_H is represented as $R_H=(h/2e^2N)\{f/[(f-1)^2+1]\}$. This assumption is apparently not valid at $B=0$. However, it gives a good approximation at $B>B_{f1}$ for the structure parameters used here. Actually, $-R_B$ (which approximately corresponds to T_{31}^2) and R_H exhibit complementary peak structures in Fig. 2. The number of subbands N in each terminal is calculated assuming a square well with infinite potential confinement as previously reported by van Houten *et al.*[18] (also see Fig. 4). It is interesting that ballistic transport characteristics observed in large structures are well explained by Landauer-equation-based analysis[7-10] in spite of the fact that $N>100$ and subband energy separation is much smaller than kT.[20] The calculated R_H characteristics are shown

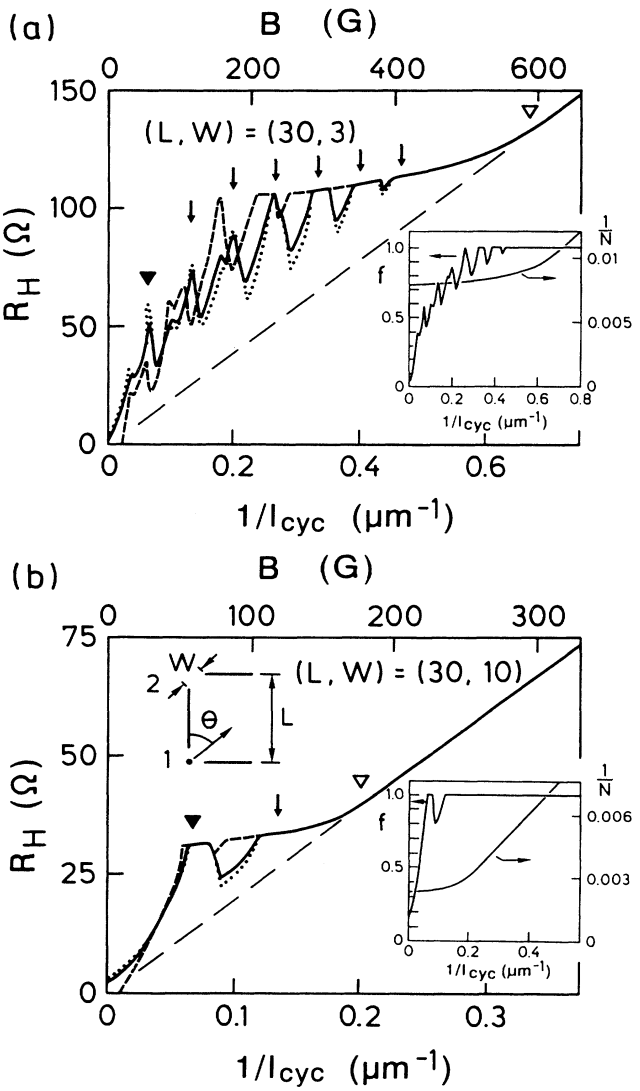

FIG. 4. Calculated R_H characteristics for (a) $(L,W)=(30,3)(\mu m)$ and (b) $(30,10)(\mu m)$. Magnetic field (B) of the horizontal axis is calculated for $E_F=9.8$ meV from $1/l_{cyc}$. Dotted, solid, and dashed lines, respectively, represent injection angular distribution of the (I1), (I2), and (I3) discussed in the text. Bottom insets show f [only for the injection (I2)] and $1/N$, and top inset of (b) shows the configuration assumed for calculating f. Solid triangles, arrows, open triangles, and fine-dashed lines indicate B_{f1}, B_{fk} (k: integer), B_w and classical linear R_H.

in Fig. 4 for $(L,W)=(30,3)$ and $(30,10)(\mu m)$. The main features of R_H are invariant with the injection distribution assumed in the calculation. R_H peaks are always obtained around focusing positions B_{fk} though peak amplitude becomes small and the oscillatory characteristic disappears at smaller magnetic fields for the collimated injections (I3). The peak amplitude is most enhanced at the third or fourth peak not at the first peak [see Fig. 4(a)]. The overlap of these peaks makes a plateaulike structure when L/W is small, as shown in Fig. 4(b). These results agree with the experimental observations in Figs. 2 and 3. This indicates that "last plateau" characteristics are well ex-

plained only by considering the focusing effect between terminals 1 and 2 for four-terminal square structures examined in this paper.

In summary, we observed R_H characteristics of ballistic four-terminal square structures, in which rounding of the shape due to depletion region spreading is negligibly small. The last plateau is always observed in R_H. It is not a plateau, but a series of focusing peaks when L/W is large; it becomes a plateaulike structure with decreasing L/W. On the other hand, quenching and negative R_H are not intrinsic to a four-terminal square structure (in other words a widened cross). When the rounding of the shape slightly collimates or shadows the injections, we can observe the quenching of R_H. On the other hand, a negative R_H is not observed without a strong collimation.

We would like to thank T. Kimura for his encouragement throughout this work and one of us (Y.H.) would like to thank K. Ploog for the stimulating support.

*Present address: Max-Planck-Institute für Festkörperforschung, 7000 Stuttgart 80, Germany.

[1]M. L. Roukes, A. Scherer, S. J. Allen, Jr., H. G. Craighead, R. M. Ruthen, E. D. Beebe, and J. P. Harbison, Phys. Rev. Lett. **59**, 3011 (1988).

[2]J. A. Simmons, D. C. Tsui, and G. Weimann, Surf. Sci. **196**, 81 (1988); C. J. B. Ford, T. J. Thornton, R. Newbury, M. Pepper, H. Ahmed, D. C. Peacock, D. A. Ritchie, J. E. F. Frost, and G. A. C. Jones, Phys. Rev. B **38**, 8518 (1988).

[3]G. Kirczenow, Phys. Rev. Lett. **62**, 2993 (1989); F. M. Peeters, *ibid.* **61**, 589 (1988); H. Akera and T. Ando, Phys. Rev. B **41**, 11967 (1990).

[4]A. M. Chang, T. Y. Chang, and H. U. Baranger, Phys. Rev. Lett. **63**, 996 (1989).

[5]C. J. B. Ford, S. Washburn, M. Büttiker, C. M. Knoedler, and J. M. Hong, Phys. Rev. Lett. **62**, 2724 (1989).

[6]M. L. Roukes, A. Scherer, and B. P. Van der Gaag, Phys. Rev. Lett. **64**, 1154 (1990).

[7]H. U. Baranger and A. D. Stone, Phys. Rev. Lett. **63**, 414 (1989).

[8]C. W. J. Beenakker and H. van Houten, Phys. Rev. Lett. **63**, 1857 (1989).

[9]C. W. J. Beenakker and H. van Houten, in *Electronics Properties of Multilayers and Low-Dimensional Semiconductor Structures,* edited by J. M. Chamberlain, L. Eaves, and J. C. Portal (Plenum, London, 1990).

[10]M. Büttiker, in *Nanostructure Systems,* edited by M. A. Reed (Academic, New York, 1990); G. Kirczenow, Phys. Rev. B **42**, 5357 (1990).

[11]C. J. B. Ford, S. Washburn, R. Newbury, C. M. Knoedler, and J. M. Hong, Phys. Rev. B **43**, 7339 (1991).

[12]G. Kirczenow and E. Castaño, Phys. Rev. B **43**, 7343 (1991).

[13]R. Behringer, G. Timp, H. U. Baranger, and J. E. Cunningham, Phys. Rev. Lett. **66**, 930 (1991).

[14]Y. Takagaki, K. Gamo, S. Namba, S. Ishida, S. Takaoka, M. Murase, K. Ishibashi, and Y. Aoyagi, Solid State Commun. **69**, 811 (1989); G. Timp, R. Behringer, S. Sampere, J. E. Cunningham, and R. E. Howard, in *Nanostructure Physics and Fabrication,* edited by M. A. Reed and W. P. Kirk (Academic, New York, 1990).

[15]L. N. Pfeiffer, K. W. West, H. L. Stormer, and K. Baldwin, Appl. Phys. Lett. **55**, 1888 (1989); C. T. Foxon, J. J. Harris, D. Hilton, J. Hewett, and C. Roberts, Semicond. Sci. Technol. **4**, 582 (1989).

[16]T. Saku, Y. Hirayama, and Y. Horikoshi, Jpn. J. Appl. Phys. **30**, 902 (1991).

[17]Y. Hirayama, T. Saku, S. Tarucha, and Y. Horikoshi, Appl. Phys. Lett. **58**, 2672 (1991).

[18]H. van Houten, C. W. J. Beenakker, J. G. Williamson, B. J. van Wees, J. E. Mooij, C. T. Foxon, and J. J. Harris, Phys. Rev. B **39**, 8556 (1989).

[19]This equation relies on exact fourfold symmetry of the device and makes the same R_H characteristics both for positive and negative magnetic field. Though some asymmetric characteristics observed in Figs. 2 and 3 indicate a slight disturbance of the fourfold symmetry in the real system, the major part of experimental results is explained by this equation.

[20]S. Tarucha *et al.* (unpublished).

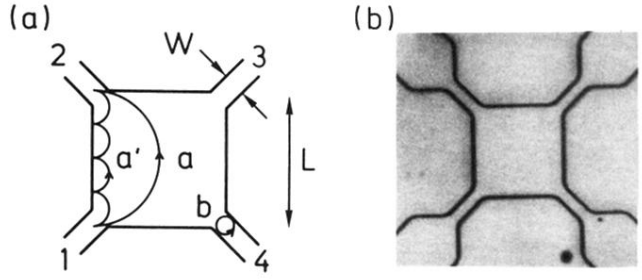

FIG. 1. (a) Schematic diagram of the high mobility four-terminal square structure. Trajectories a, a', and b correspond to B_{f1}, B_{fk} $(k=4)$, and B_w. They are discussed in the text. (b) Optical micrograph of $(L,W)=(30,4.4)(\mu\text{m})$ sample.

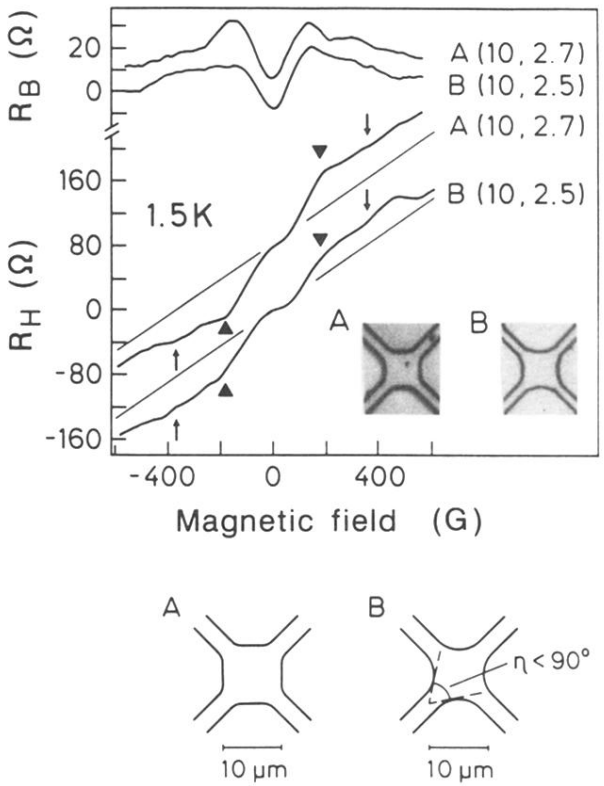

FIG. 3. R_H and R_B characteristics of $L = 10\ \mu$m structures; A is a typical structure and B is an intentionally rounded structure. An optical micrograph of each structure is shown in the figure; bottom inset indicates a schematic drawing. Solid triangles, arrows, and fine-straight lines indicate B_{fl}, B_{fk} $(k = 2)$, and classical linear R_H. The R_H curves are offset vertically by 80 Ω and the R_B curves are offset by 20 Ω for clarity.